

# PROCESSING MERGED AEROMAGNETIC DATA, CENTRAL LABRADOR, TO ASSIST WITH BEDROCK MAPPING, AND MINERAL-DEPOSIT IDENTIFICATION

M. Arshian  
Terrain Sciences and Geoscience Data Management Section

## ABSTRACT

*This study focuses on the processing and enhancement of merged aeromagnetic datasets from central Labrador to improve the resolution, and hence the interpretation, of magnetic anomalies for geological mapping and structural analysis. After applying reduction to the pole (RTP) transformations, derivative and tilt-angle analyses further refined the identification of geological structures. Subsequent application of filtering techniques includes high-pass, low-pass and combined filters that were used to distinguish shallow- and deep-magnetic sources. The use of hybrid grids, which integrate multiple enhancements, enable detailed visualization of complex features such as folds and faults that can assist with bedrock mapping and interpretation. These advanced methods revealed significant geological patterns across various depths, providing detailed insights into the region's subsurface structures and their tectonic context.*

## INTRODUCTION

High-sensitivity aeromagnetic data from eight overlapping areas, across central Labrador, were recently assessed. Minor offsets in individual survey areas were evaluated, levelled and merged into a consistent and seamless database (M. Arshian and G. Kilfoil unpublished data, 2025).

This study aims to improve the merged aeromagnetic data from Labrador, employing data enhancement techniques to improve visual contrasts to facilitate the identification of key magnetic variations. These methods highlight specific sources of magnetization and reveal critical geological features, improving the interpretation of subsurface structures and mineral deposit identification.

## LOCATION

The eight surveyed sites across central Labrador include the following areas from east to west – 1) Makkovik River East, 2) Makkovik River West, 3) Hopedale, 4) Mistassin Lake, 5) Schefferville East (Lake Ramusio), 6) Schefferville Centre, 7) Schefferville West (Lake Attikamagen), 8) Shabogomo Lake – represent key regions for aeromagnetic analysis. Surveys 4–8 also cover part of eastern Québec. Figure 1 illustrates the location and extent of these surveyed areas.

Figure 2 illustrates the simplified bedrock geology, contact and fault maps that correspond to the Labrador portion

of the surveyed areas (Wardle *et al.*, 1997). The different characteristics of the aeromagnetic surveys across the eight study areas are summarized in Table 1.

The eight separate surveys were levelled and stitched together to create a unified levelled grid, as shown in Figures 3 and 4.

## METHODS

After generating the integrated total magnetic intensity (TMI) dataset, gridding is a crucial step for subsequent processing. Gridding is an interpolation technique that transforms irregularly spaced measurement points into a square uniform structured dataset. Magnetic field data is typically gridded using minimum curvature methods, with grid cells about 1/4 or 1/5 the spacing of survey lines (Briggs, 1974; O'Connell *et al.*, 2005; O'Connell and Owers, 2008).

## IGRF CORRECTION

Once a reliable grid is created, the International Geomagnetic Reference Field (IGRF) (Alken *et al.*, 2021) – a global model of Earth's magnetic field – is subtracted from the measured data total magnetic intensity (TMI). This correction highlights local magnetic variations caused by crustal sources. After gridding, levelling and compiling the data, enhancements like IGRF correction become essential for accurately interpreting geological features. Following IGRF correction, all data processing is applied to the RMI grid.

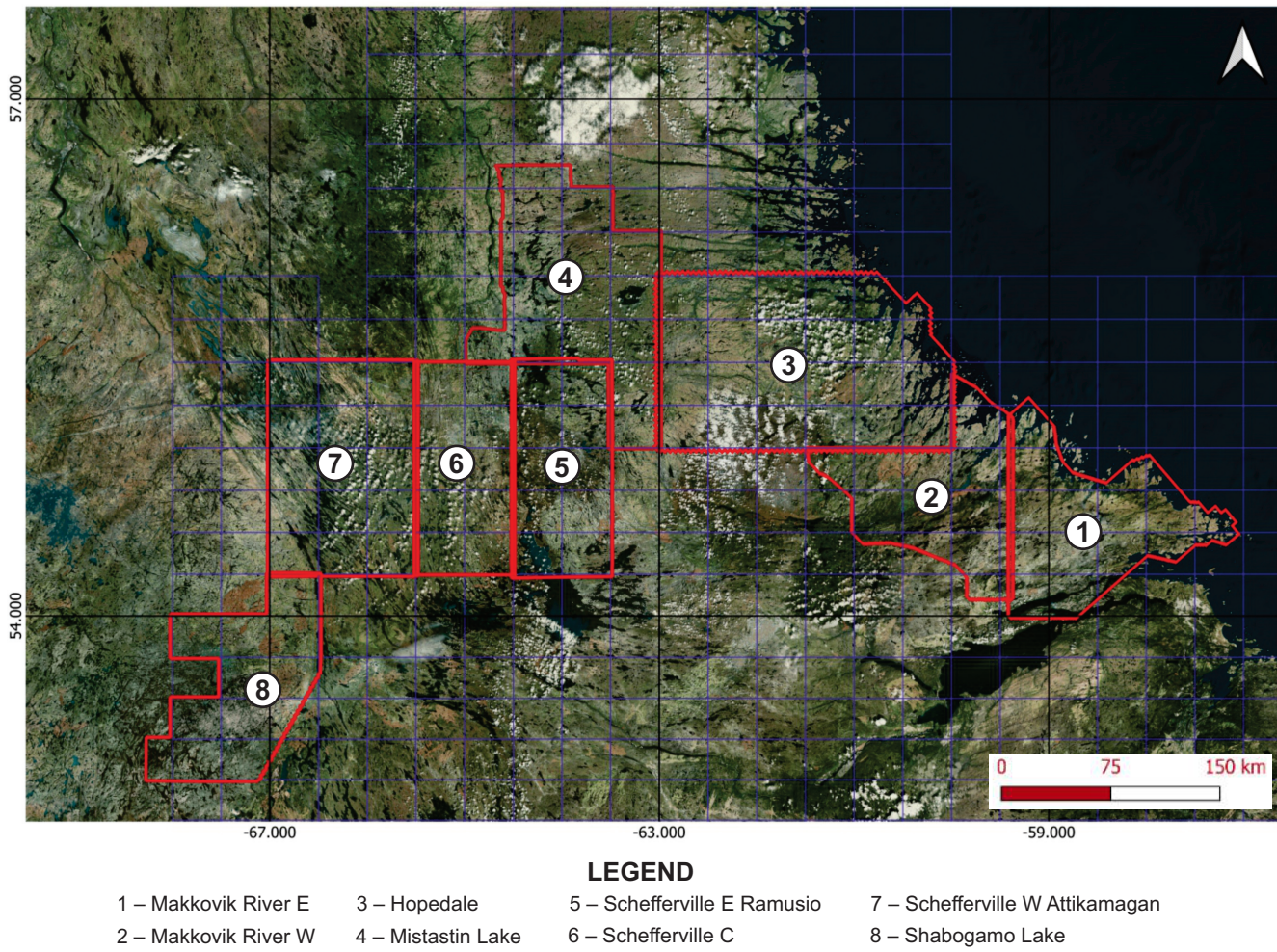


**Figure 1.** Airphoto of the eight surveyed areas, central Labrador.

## IMAGE DISPLAY OF MAGNETIC FIELD DATA

Magnetic field data visualization plays a crucial role in interpreting geological information. Unlike gravity data, magnetic data exhibit sharper variations, with much of the amplitude range in small datasets. Thus, to improve clarity, histogram equalized colour stretches are commonly employed, ensuring that each colour band covers an equal area and enhancing detail representation. Another effective technique is sun shading, where simulated lighting adds shadows and highlights on the data surface. This approach accentuates subtle features and shorter wavelength variations. Typically, the light source is set at moderate or low angles to emphasize features perpendicular to the illumination direction, while parallel lighting can help minimize levelling errors (the most common directional filter). Presenting data on two or three grid compositions would be another viewing technique to accentuate some features better, which will be detailed in subsequent sections.

## PROCESSING OF GRIDS (SPACE DOMAIN AND WAVENUMBER DOMAIN)

The data can be processed in either the spatial domain or the wavenumber domain. In aeromagnetic surveys, measurements of the magnetic field at various locations on Earth's surface are collected in the spatial domain. In contrast, the frequency domain or (wavenumber domain) represents data in terms of spatial frequency, showing how often variations occur over a given distance. Processing grids in the wavenumber domain (also called the Fourier domain) includes analyzing data based on wavelength. Low-wavenumber components, correspond to long wavelengths (1/wavelength) or near-DC signals, while high-wavenumber components represent shorter wavelengths.

The Fourier transform bridges the two domains (the spatial domain or the wavenumber domain), enabling efficient data processing by fast Fourier transform (FFT) oper-

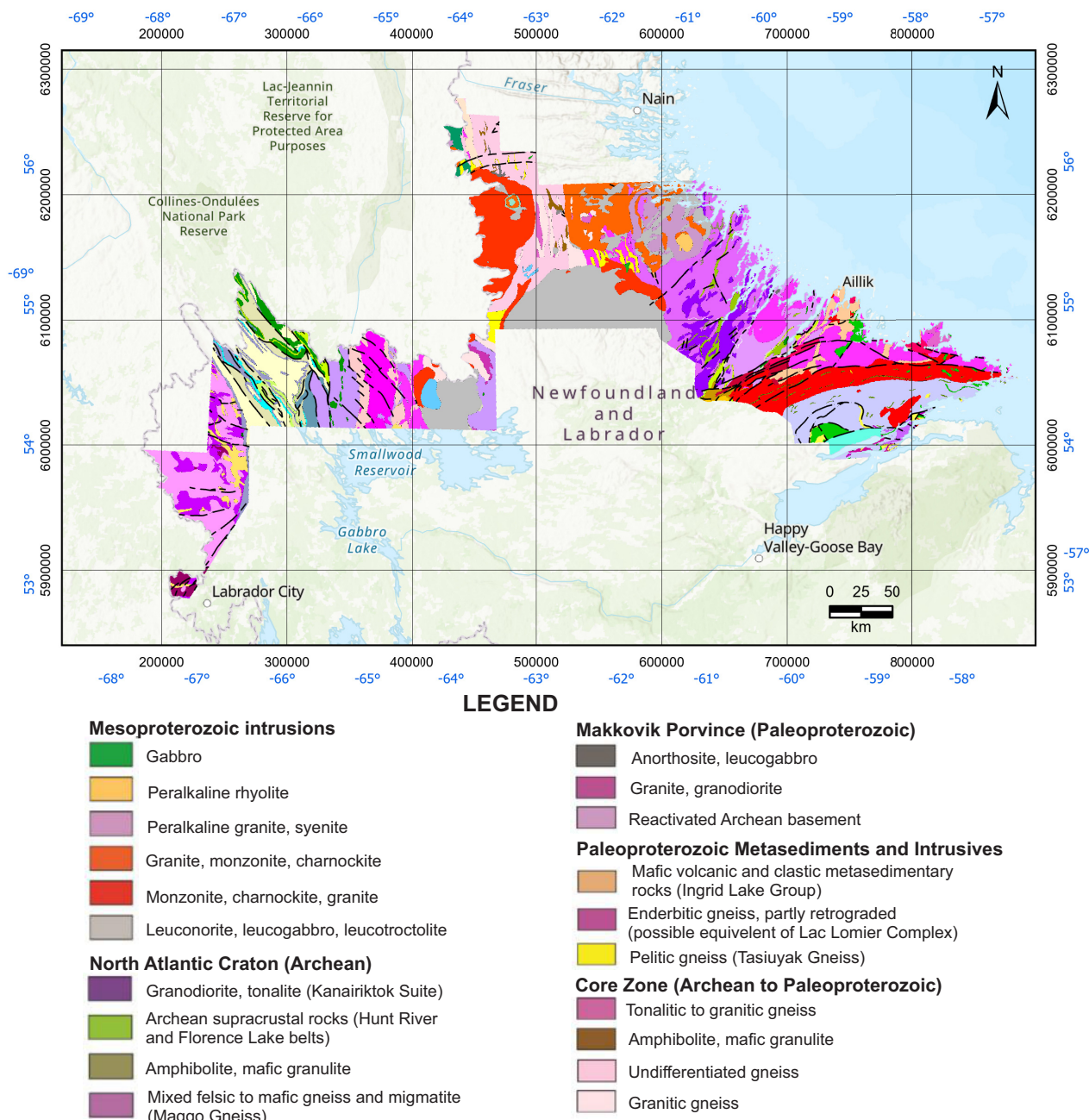


**Figure 2.** Simplified bedrock geology, contacts and faults maps of the surveyed areas, central Labrador (after Wardle *et al.*, 1997).

ations. This allows analysts to apply filters and enhancements with precision, such as noise reduction or feature enhancement, in the frequency domain.

A simplified summary of some processing applied to the merged dataset in wavenumber domain is as follows.

#### Reduction to the Pole (RTP) Transform

Reduction to the pole (RTP) is an essential technique which, in most cases, provides imagery that more accurately

represents the geometry of magnetic rock formations compared to total-magnetic-intensity data. Using the RTP transformation is essential for interpreters (Isles and Rankin, 2013). Campbell *et al.* (1992) provide examples demonstrating that RTP is practical in most scenarios.

Magnetic anomalies vary with latitude, with a greater distortion arising closer to the equator (Jessell, 2001). Thus, before processing magnetic data for structural studies or geological mapping, the effects of the orientation of the Earth's magnetic field on anomalies must be corrected. The

**Table 1.** Characteristics of aeromagnetic surveys across central Labrador that were merged in this project

Survey area	Line spacing/ direction	Projection of data	Survey Date	Methods (mag/rad)	Altitude (terrain clearance)	Grid cell size
1 Makkovik River E	Traverse: 200 m, Az: 135° Tie: 1200 m, Az: 045°	NAD83, UTM Zone 20	July–Sept. 2023	Total field mag; Radiometric	80 m	50 m
2 Makkovik River W	Traverse: 200 m, Az: 135° Tie: 1200 m, Az: 045°	WGS84, UTM Zone 20	Aug.–Oct. 2022	Total field mag; Radiometric	146 m	50 m
3 Hopedale	Traverse: 200 m, N 135° E Tie: 1200 m, N 45° E	WGS84, UTM Zone 20	Jan.–Aug. 2018	Total field mag;	100 m	50 m
4 Mistastin Lake	Traverse: 200 m, Az: 090°; Tie: 1200 m, Az 000°	WGS84, UTM Zone 20	Feb.–April 2012	Total field mag	80 m	50 m
5 Schefferville E Lake Ramusio	Traverse: 200 m, Az: 000°; Tie: 1200 m, Az 090°	NAD83, UTM Zone 20	May–Aug. 2009	Total field mag; Radiometric	80 m	50 m
6 Schefferville C	Traverse: 200 m, Az: 090°; Tie: 1500 m, Az 000°	NAD83, UTM Zone 20	Feb.–Mar. 2009	Total field mag; Digital Terrain model	90 m	50 m
7 Schefferville W Lake Attikamagan	Traverse: 200 m, Az: 045°; Tie: 1200 m, Az 135°	NAD83, UTM Zone 20	May–Sept. 2009	Total field mag; Radiometric	80 m	50 m
8 Shabogamo Lake	Traverse: 300 m, Az: 090°; Tie: 1800 m, Az 000°	NAD83, UTM Zone 19	Feb.–Mar. 2011	Total field mag	80 m	70 m

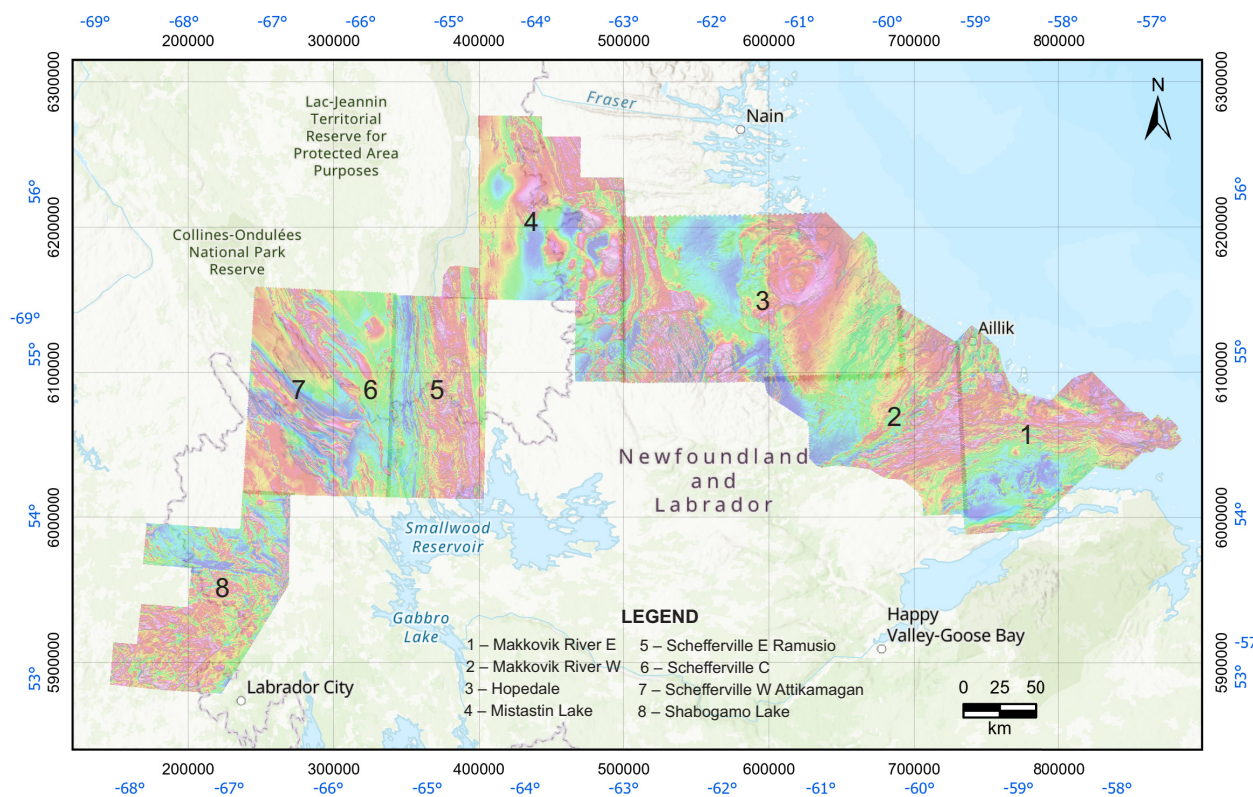


**Figure 3** Aeromagnetic survey grids of eight areas (1-8) across the central Labrador, before merging.

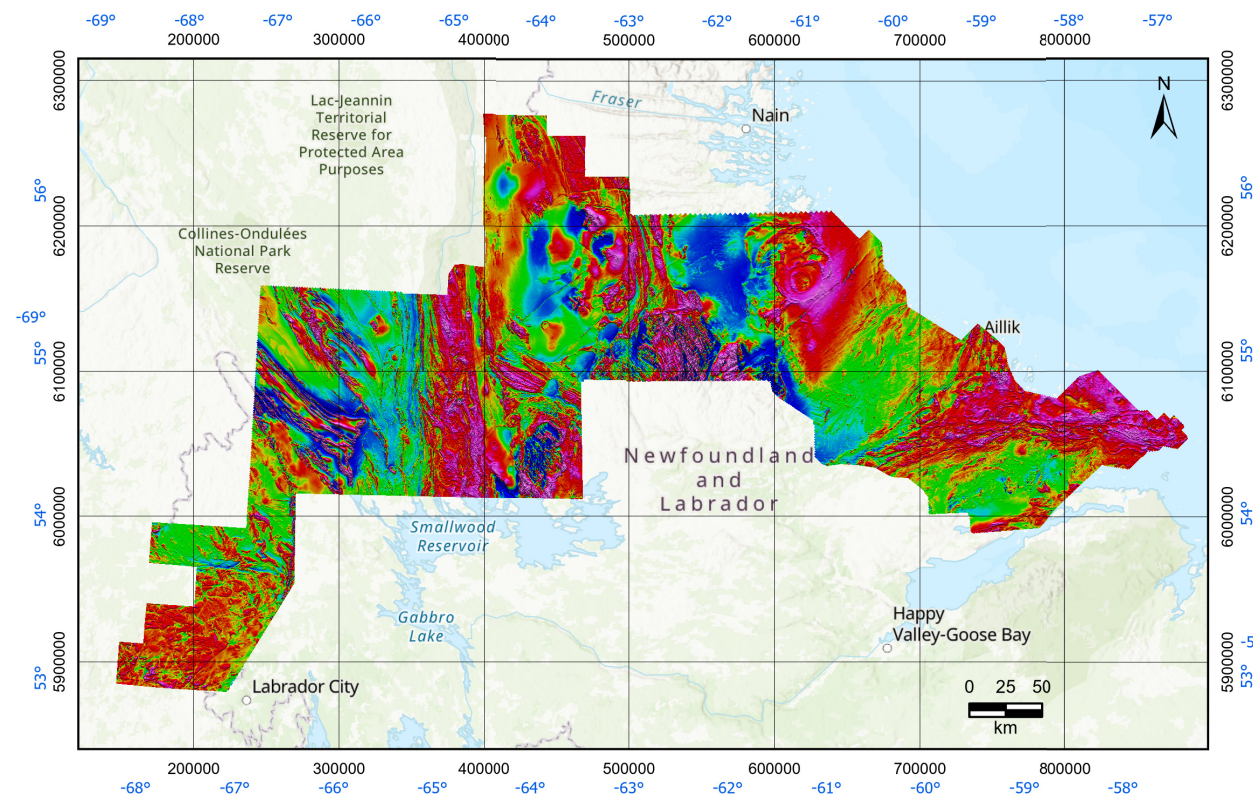


**Figure 4.** A unified levelled grid by stitching eight grids.

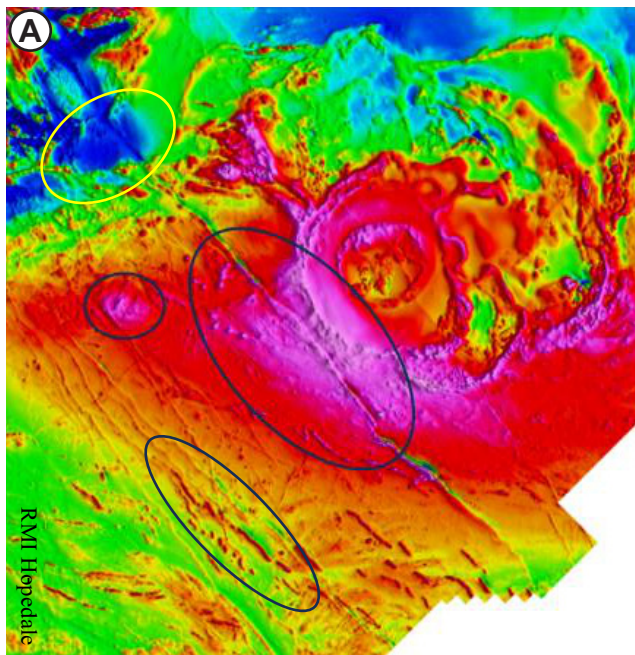
reduction to pole transform adjusts magnetic data to simulate how it would appear if measured at the geomagnetic poles ( $I = 90^\circ$ ), where the Earth's magnetic field inclination is  $90^\circ$  (see Macmillan, 2011). At the poles, magnetic anomalies are typically positive and centred over the magnetic sources.

While RTP is a useful tool for magnetic-data interpretation, it has limitations in specific scenarios. It assumes all magnetization aligns with the Earth's field, which may not hold in areas with significant remanent magnetization, where the magnetization direction is unknown or non-uniform. Hence, in these complex environments, other techniques, such as the Analytic Signal transformation can complement RTP. Low-magnetic-field inclinations pose another challenge for RTP due to numerical instability, which can introduce artifacts. Proper line spacing and advanced numerical methods can mitigate these issues, enabling RTP to remain a critical tool for structural analysis.

Central Labrador's local inclination is around  $75^\circ$  (high-magnetic inclination), with less distortion from the magnetic field in the North Pole. So, in this area, RTP was effectively applied using FFT to transform local magnetization with the geomagnetic field at the North Pole, as illustrated in Figure 5.

### Regional-residual Separation

Potential fields, such as the Earth's magnetic field, often include contributions from various crustal sources.



Separating overlapping signals, known as regional-residual separation, and involves distinguishing local, sharp anomalies (residuals) from broader, smoother variations (regional fields) caused by deeper or more distant sources. This interpretive process is nonunique and relies on identifying differences in the character of the fields. So, applying different filters to the merged dataset helps achieve effective separation and improve the clarity of the analysis.

### Bandpass Filters

In data processing, filtering reduces undesirable signal components while increasing or maintaining beneficial ones. The main purpose of filtering in aeromagnetic surveys is to improve the interpretation of the data by differentiating between deeper and shallower components. Bandpass filtering can be used to highlight magnetic sources at specific depths by leveraging the relationship between depth and wavelength. High-pass filtering enhances shallow sources by suppressing deeper ones, while low-pass filtering does the opposite. However, bandpass filters do not perfectly isolate magnetic fields from different sources, making them unsuitable for precise modelling or inversion studies (Foss, 2020).

### High-pass Filters

High-pass filters, which have shorter wavelengths and smaller spatial variations, enhance near-surface structures by allowing higher frequency signals to pass through, while attenuating lower frequency signals. These filters are partic-

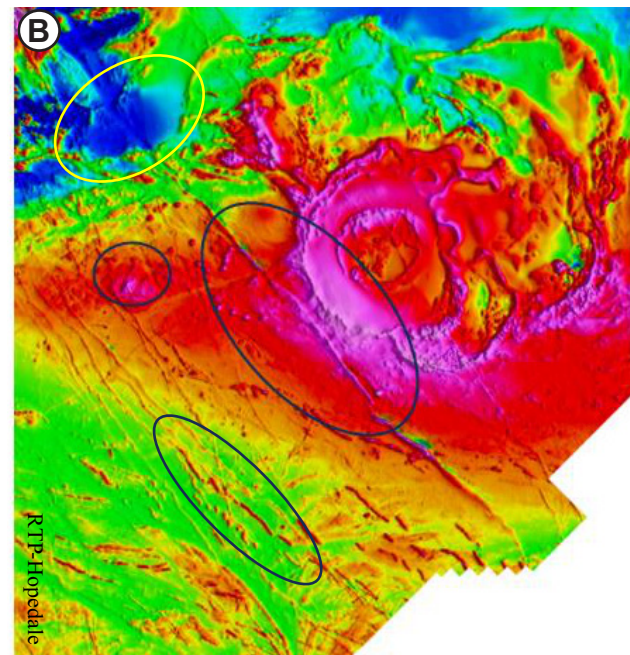


**Figure 5.** Comparison between A) the RMI and B) the RTP grids of the Hopedale area, Labrador, Canada. The high magnetic signatures become more symmetrical and shifted slightly northward in RTP image. Several examples are outlined.

ularly effective in highlighting shallow sources in hard rock terrains. The short-wavelength aeromagnetic data for central Labrador, enhanced with high-pass filters, accentuates shallow structures (Figure 6).

The fine details of folds in the Southeastern Churchill Province, as seen in Figure 7 are not evident at all in RMI-RTP or 1VD images of the same dataset (Geological Survey of Newfoundland and Labrador, 2013; Butler, 2019).

### Low-pass Filters

Low-pass filters are simpler to apply than high-pass filters because they suppress fine details instead of enhancing them. Their purpose is to highlight deeper sources while minimizing the influence of shallow ones. These filters are particularly useful for studying deep basement structures that may be hidden beneath shallow magnetic layers, such as younger volcanic flows (Isles and Rankin, 2013). They also help suppress surface magnetic sources, like subglacial sediment (till) that cover shallow bedrock. In essence, low-pass filters focus on deeper geological features by reducing interference from near-surface materials, however, this filter cannot perfectly isolate magnetic fields from shallower sources such as highly magnetic iron formations that are near the surface.

Figures 8 and 9 show how the enhanced long-wavelength aeromagnetic dataset (low-pass wavelength) extracts deep crustal components of the merged dataset, providing far more detailed structural information than the TMI image.

## DERIVATIVES

### First Vertical Derivative

The first vertical derivative (1VD) has traditionally been the most popular high-pass filter commonly used in aeromagnetic surveys due to its computational efficiency, reliable results, and easy interpretability in relation to magnetic rock bodies (Isles and Rankin, 2013). The 1VD filter is unbiased in any direction, *i.e.*, this filter only responds to vertical intensity changes without being influenced by directional trends that might arise from other filtering methods. This makes it especially useful for identifying faults, contacts, and thin magnetic sources without creating extra artifacts or directional bias. It preserves peak positions from TMI or RTP while retaining narrower anomalies that more accurately represent the width of the magnetic rock body. The calculated first vertical derivative is commonly used in an attempt to accentuate near-surface features while suppressing deeper ones, improving the resolution of closely

spaced sources and improving structural and lithological interpretation (see Figures 10 and 11).

### Tilt Angle

The tilt angle, determined by the arctangent of the first vertical derivative divided by the total horizontal gradient, is a robust tool for identifying geological contacts, faults, and shear zones (Miller and Singh, 1994).

$$\text{Tilt of TMI} = \tan^{-1} \left( \frac{\partial \text{TMI}}{\partial z} \right)$$

$$\text{Where } \frac{\partial \text{TMI}}{\partial h} = ((\partial \text{TMI} / \partial x)^2 + (\partial \text{TMI} / \partial y)^2)^{1/2}$$

$h$  = location along a horizontal axis perpendicular to the contact

$z$  = contact depth

By substitution of the gradients, we get:

$$\theta = \tan^{-1} [h/z]$$

For each anomaly, tilt angle ranges away from  $+90^\circ$  over the top of a vertical mass to  $-90^\circ$  at infinity sway from the body. Directly above the point where a magnetic source and the surrounding rock make contact is the  $0^\circ$  angle line and represents a phase angle between a vertical and horizontal vector (Zengerer, 2018). This enables a more accurate estimation of source locations (after RTP transform).

The tilt angle is an effective method to enhance the interpretation of magnetic data by defining the edges of geological features. It provides a reliable means of mapping vertical contacts and offers improved clarity for both shallow- and deep-anomaly sources. It equally represents both strong and weak sources from varying depths. This can make it challenging to isolate and identify individual magnetic rock units while accurately depicting lithological contacts with varying dips (Cooper and Cowan, 2006).

The tilt angle for the Labrador total-merged dataset was generated in greyscale to facilitate advanced enhancement methods in subsequent processing stages (Figure 12).

### UPWARD CONTINUATION

Upward continuation is a low-pass filtering method that emphasizes broader, regional features while diminishing finer, high-frequency details.

To achieve upward continuation, the wavenumber domain filter is given by the equation:  $F(\omega) = e^{-h\omega}$  where  $h$

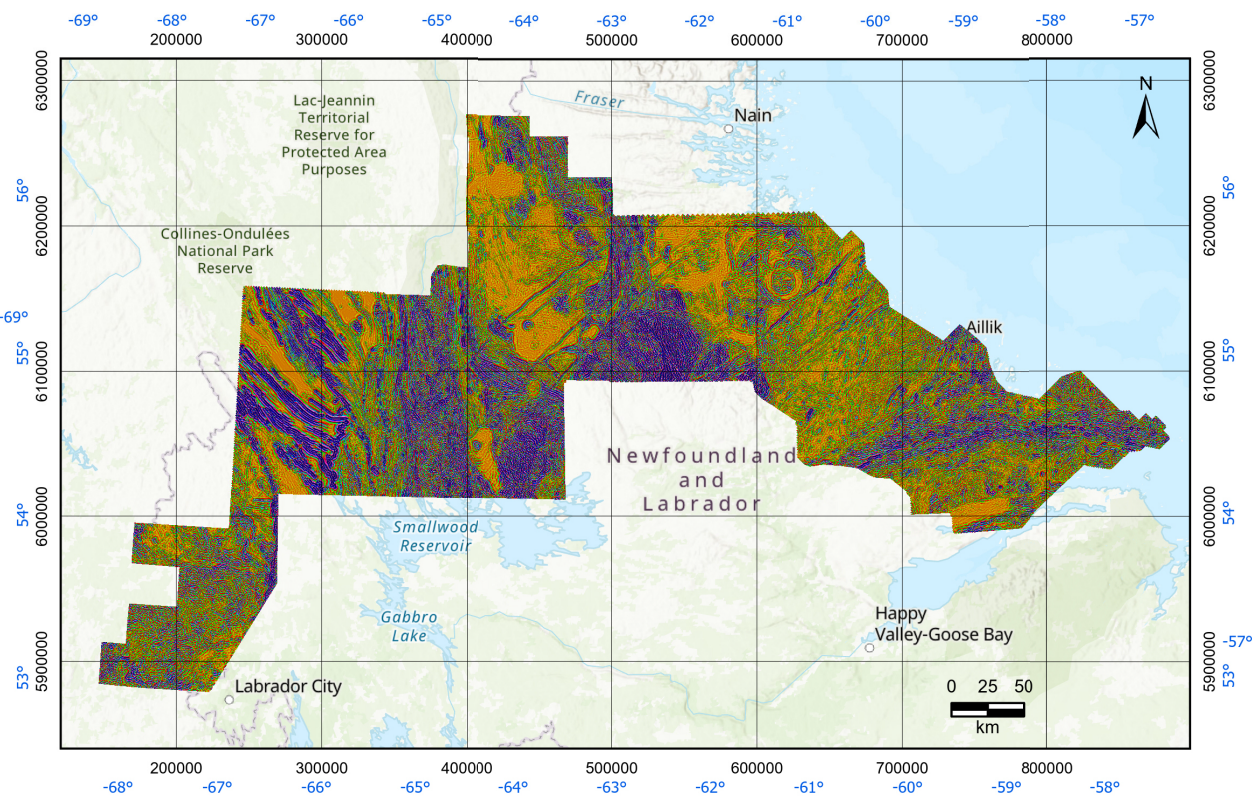


**Figure 6.** Short-wavelength aeromagnetic data enhanced with high-pass filter, Total merged grid, Labrador.

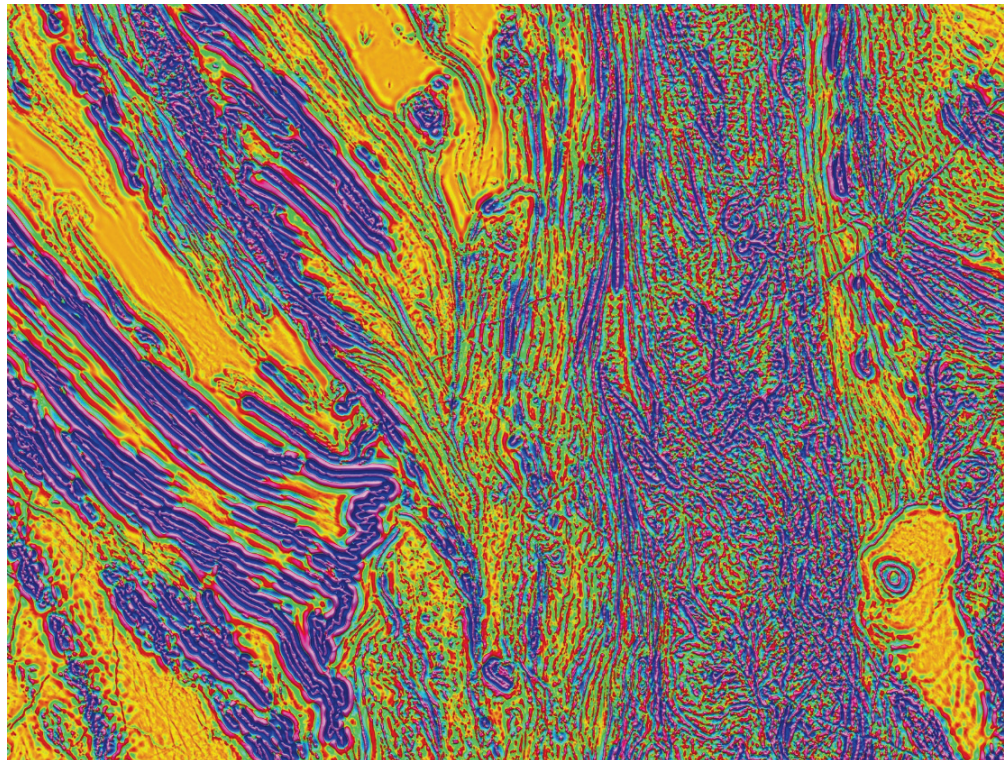


**Figure 7.** Short-wavelength components of the aeromagnetic data enhances fine details of folds in the Southeastern Churchill Province.

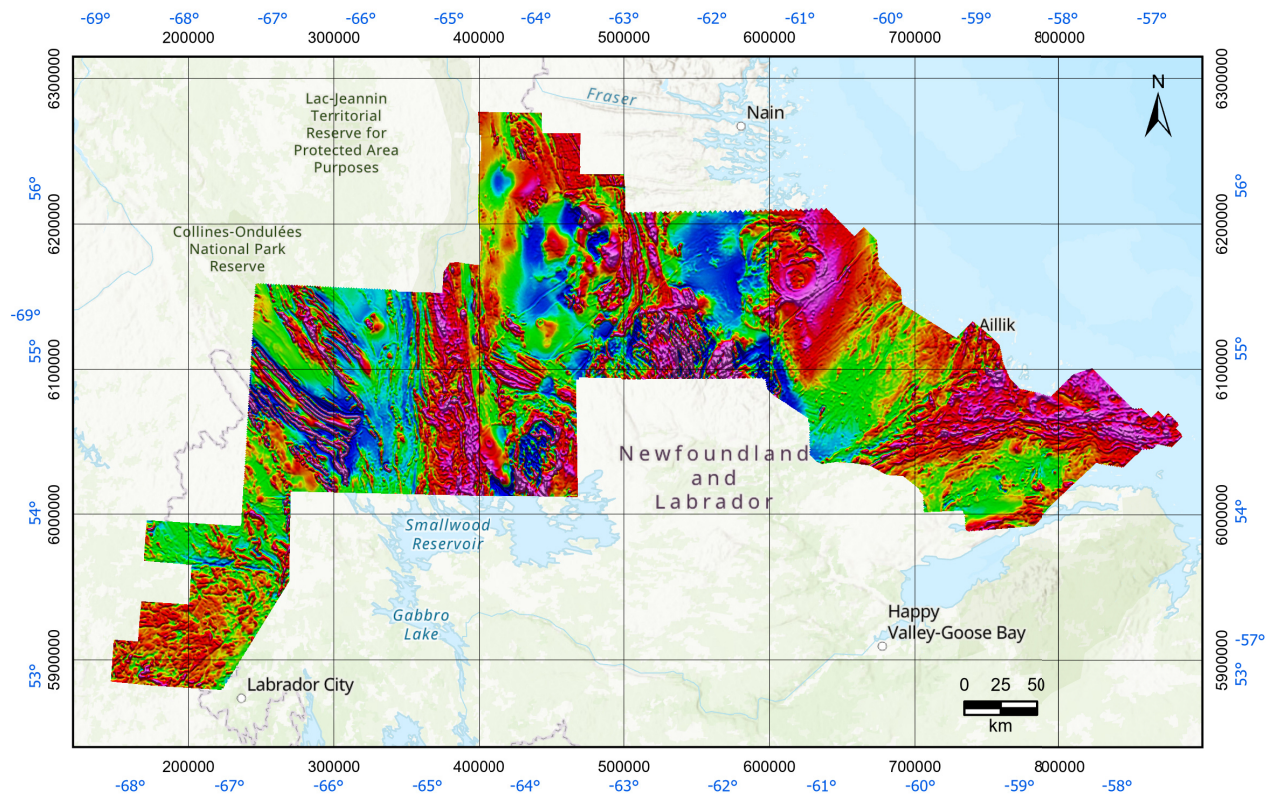


**Figure 8.** Long-wavelength components of the aeromagnetic data enhance the deeper structures for the merged data of Labrador.

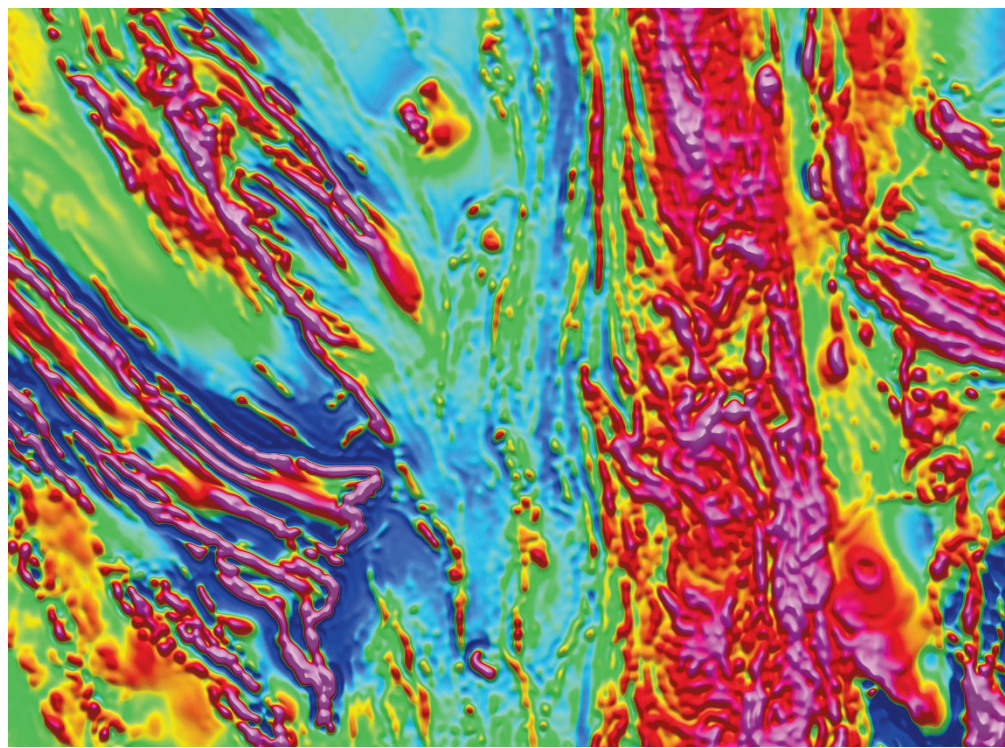


**Figure 9.** Long-wavelength components of the aeromagnetic data enhance the deeper structures for the merged data of Labrador.

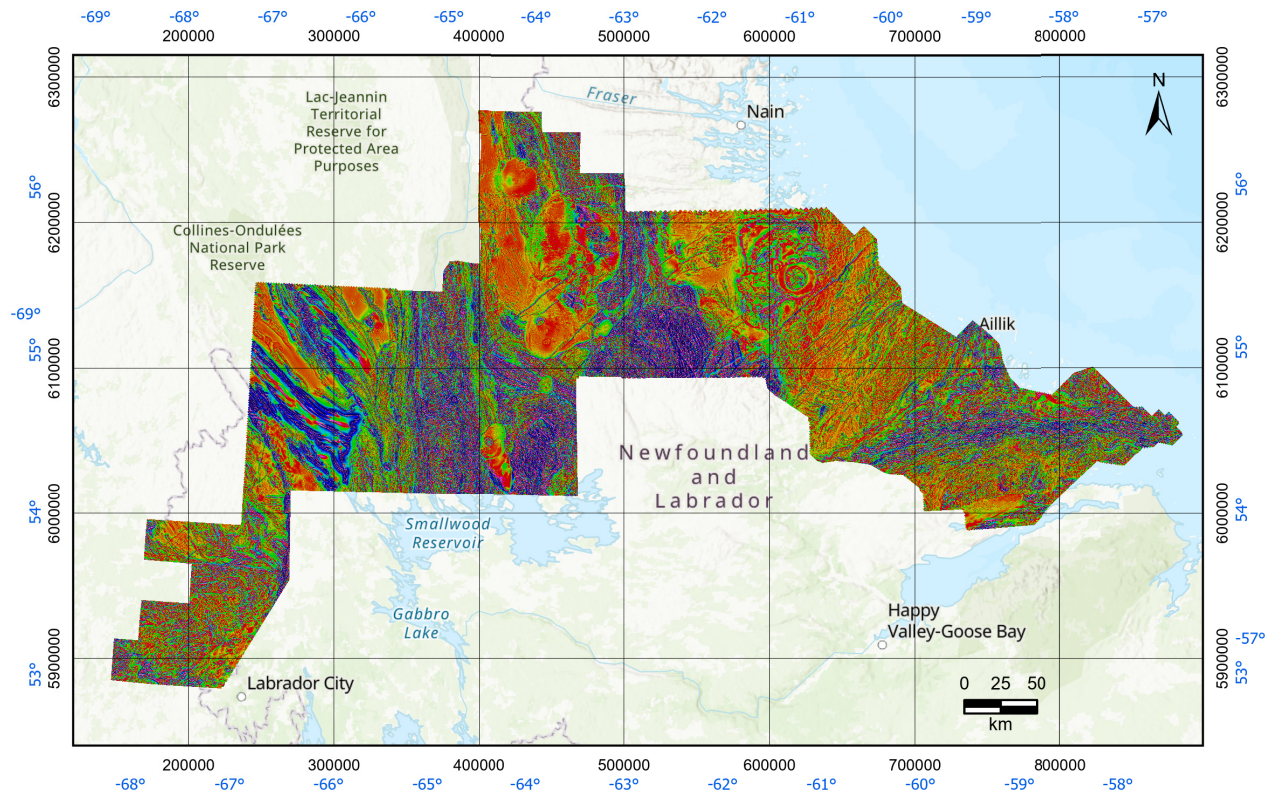


Figure 10. The first vertical derivative of the total merged grid, Labrador.

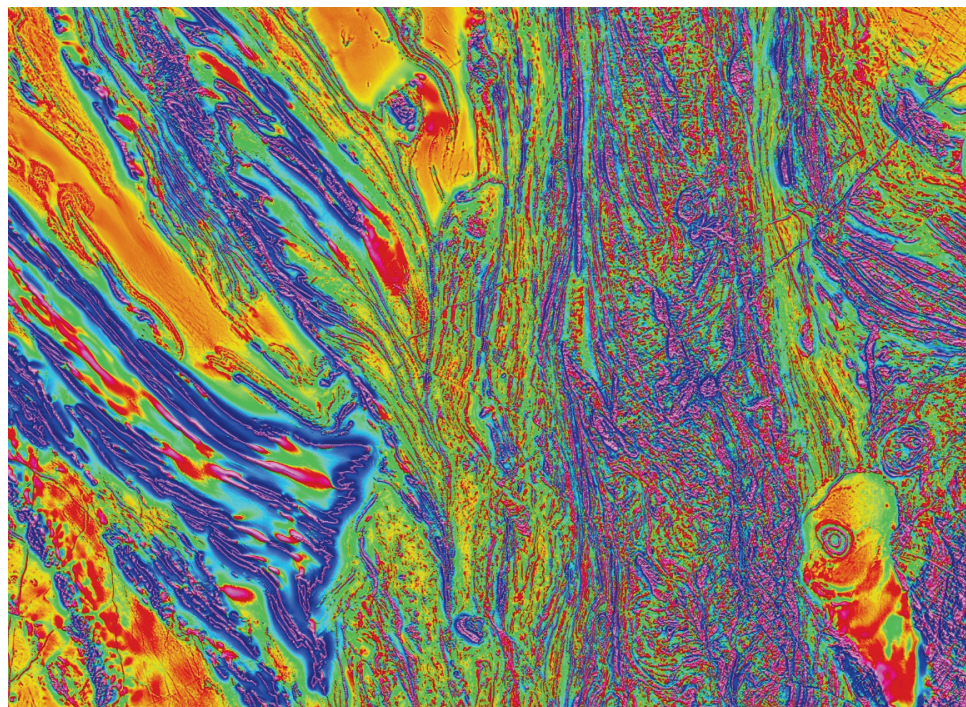
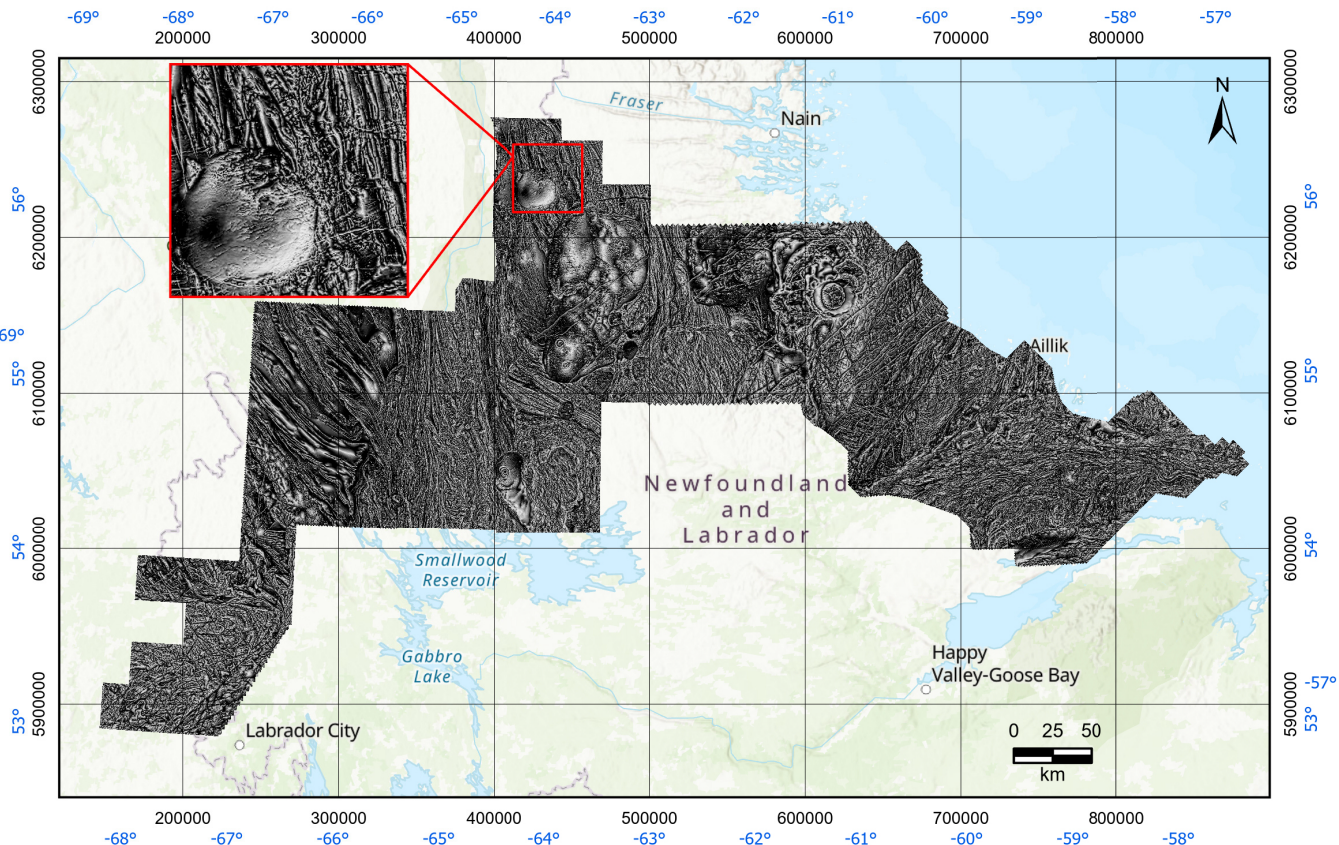


Figure 11. The calculated first-vertical derivative of the Southeastern Churchill Province, Labrador, enhances shallow sources and provides a better resolution of closely spaced sources.



**Figure 12.** The greyscale tilt angle of the total-merged grid for Labrador was generated to depict the linier pattern as well as the strong and weak sources equally.

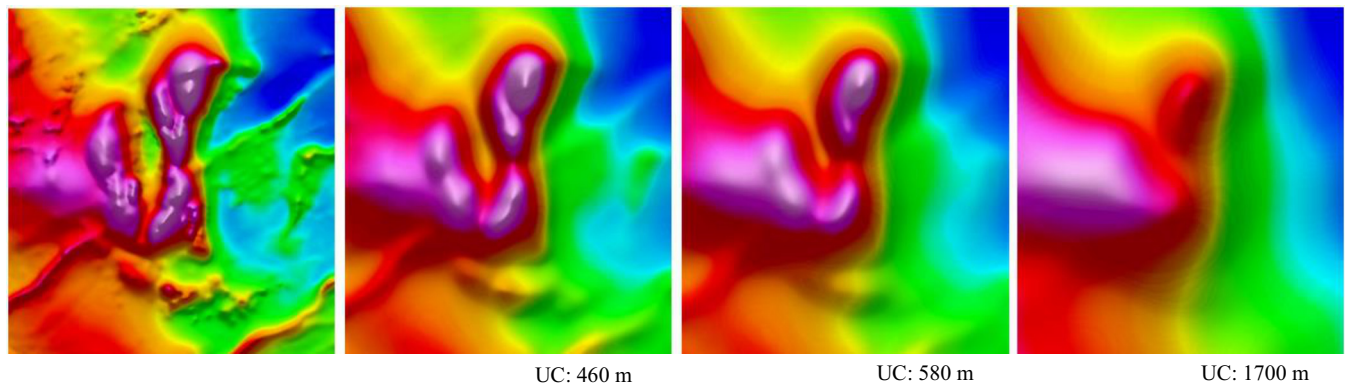
represents the continuation height. This function progressively decays as the wavenumber increases, effectively reducing the influence of higher wavenumbers (1/wavelength). The greater the distance between the detector from the source, the lower the resolution and amplitude of data, with only the longer wavelength and deeper features remaining (Figure 13).

Spector and Grant (1970) first demonstrated its application to sedimentary-basin interpretation, with subsequent studies by Morgan (1998) and Cowan and Cowan (1993) reinforcing its effectiveness. Figure 13 shows RMI grids and upward continuation at different heights, highlighting how this method extracts depth-specific information. What makes this method unique is its ability to standardize the measurement heights of different surveys. For example, low-level surveys can be adjusted upward to match higher altitude ones, ensuring seamless merging. This technique offers combined aeromagnetic surveys of varying resolution

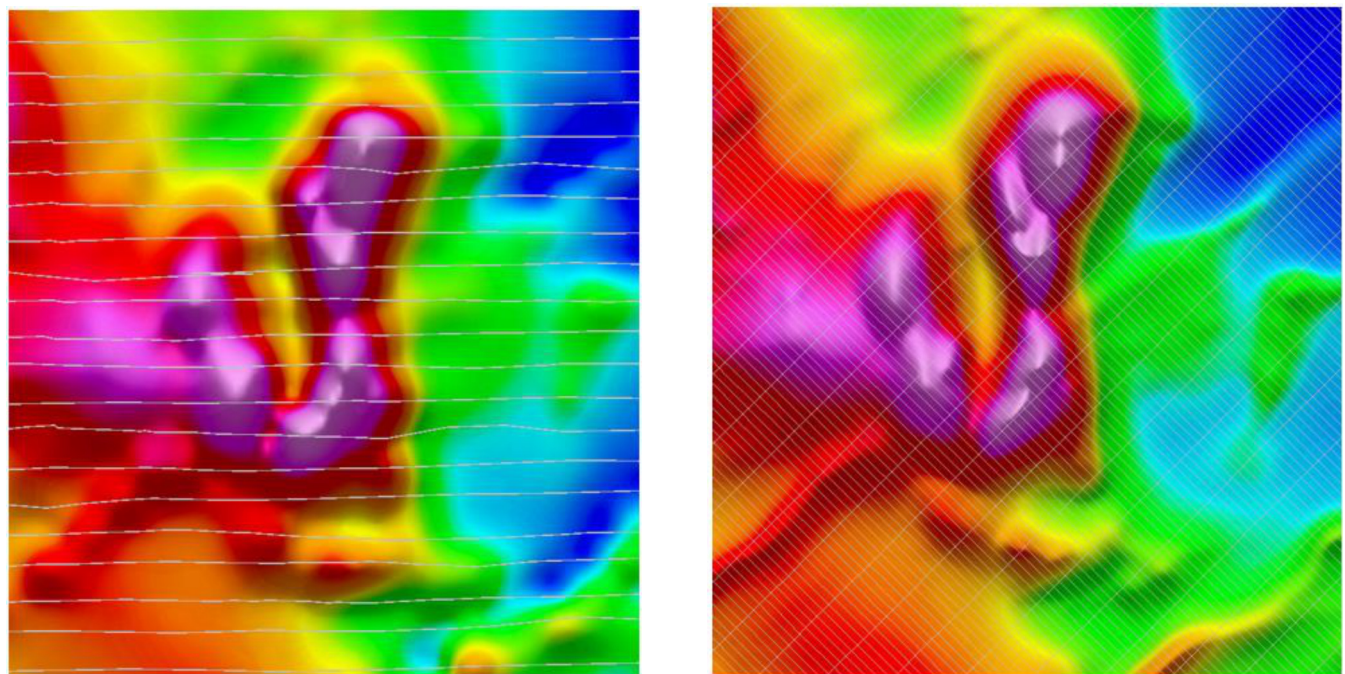
and survey altitude, as shown in the creation of global aeromagnetic maps (Korhonen *et al.*, 2007).

Figure 14 compares the regional data with the 200-m upward-continued residual data of part of the Hopedale Block (NTS 13M/16 and 13M/04) in Labrador, covering the same area as Figure 13. The regional survey was flown by the Geological Survey of Canada at an altitude of approximately 300 m, with a flight line spacing of 800 m and gridded to 150 m. In contrast, the recent high-resolution survey (Coyle, 2019), was flown at a lower altitude of 100 m, with a flight line spacing of 200 m and a finer gridding resolution of 50 m.

To ensure compatibility for levelling and merging, the Hopedale survey data was raised by 200 m from its original 100 m altitude above the ground. This adjustment aligns it more closely with the regional grid, allowing for more meaningful comparison and integration of the datasets.



**Figure 13.** RMI grid and upward continuation for three different heights show how this filter can extract information for different depths by progressively increasing the continuation height. The method effectively removes high-frequency anomalies from shallow sources, enhancing the response from deeper structures.



**Figure 14.** Comparison of the regional data with the survey altitude of approximately 300 m above the ground and flight-line spacing of 800 m, gridding to 150 m, with the recent 200 m upward continued residual data, the 200 m flight-line spacing data, and gridding to 50 m (NTS 13M/16), Hopedale Block.

## COMBINED GRIDS IMAGERY

Geological structures and features occur across a wide range of scales, from regional faults spanning kilometres to localized features a few metres wide. In unprocessed magnetic data, signals from different depths and scales overlap, making it challenging to isolate meaningful patterns. The combination of low-pass and high-pass effectively separates near-surface and deeper sources in the same image, reducing ambiguity.

## HYBRID VIEWING

Combining data from two or three grids into a hybrid grid can accentuate features better than on single grids. By combining residual grids in colour with shaded-relief representations, such as the greyscale tilt derivative, a hybrid viewing is created. This technique modulates colour intensity with the derivative value, highlighting subtle linear structures not apparent in the residual map alone.

Figure 15 demonstrates the comparison of a hybrid grid and the RMI grid for the merged Makkovik W-E region, showcasing enhanced linear details in the hybrid grid.

#### HIGH-PASS AND TILT ANGLE OF LOW-PASS INTEGRATION

Combining high-pass filtering with the tilt angle of low-pass data enhances both shallow and deep geological features. The method begins by isolating short-wavelength components (high-pass filter) to highlight near-surface structures while removing long-wavelength signals. Subsequently, the tilt angle of the long-wavelength (low-

pass) data is added back as greyscale, restoring the broader regional context without overpowering the near-surface features (Figure 16). This ensures that both local and large-scale geological contexts are visible in the same dataset, supporting more comprehensive understanding of the geological features (Figure 17).

#### LOW-PASS, HIGH-PASS AND TILT ANGLE OF LOW-PASS INTEGRATION

To further refine the visualization, the low-pass grid (in colour and histogram-equalized stretch) was superimposed onto the combined grid (high-pass and tilt angle of low-

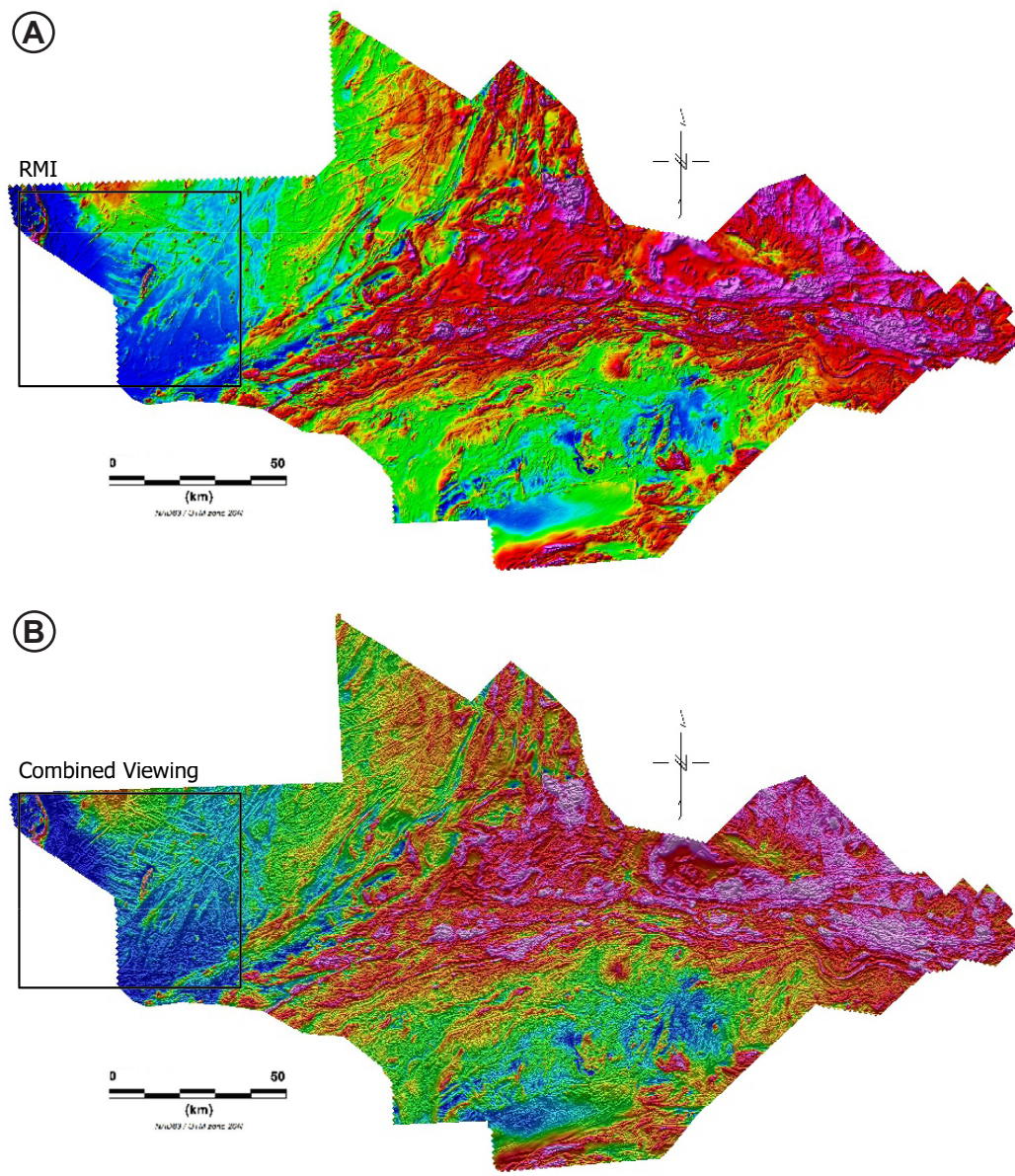


**Figure 15.** Comparison of A) the RMI grid and B) the combined hybrid viewing for the merged Makkovik W-E.

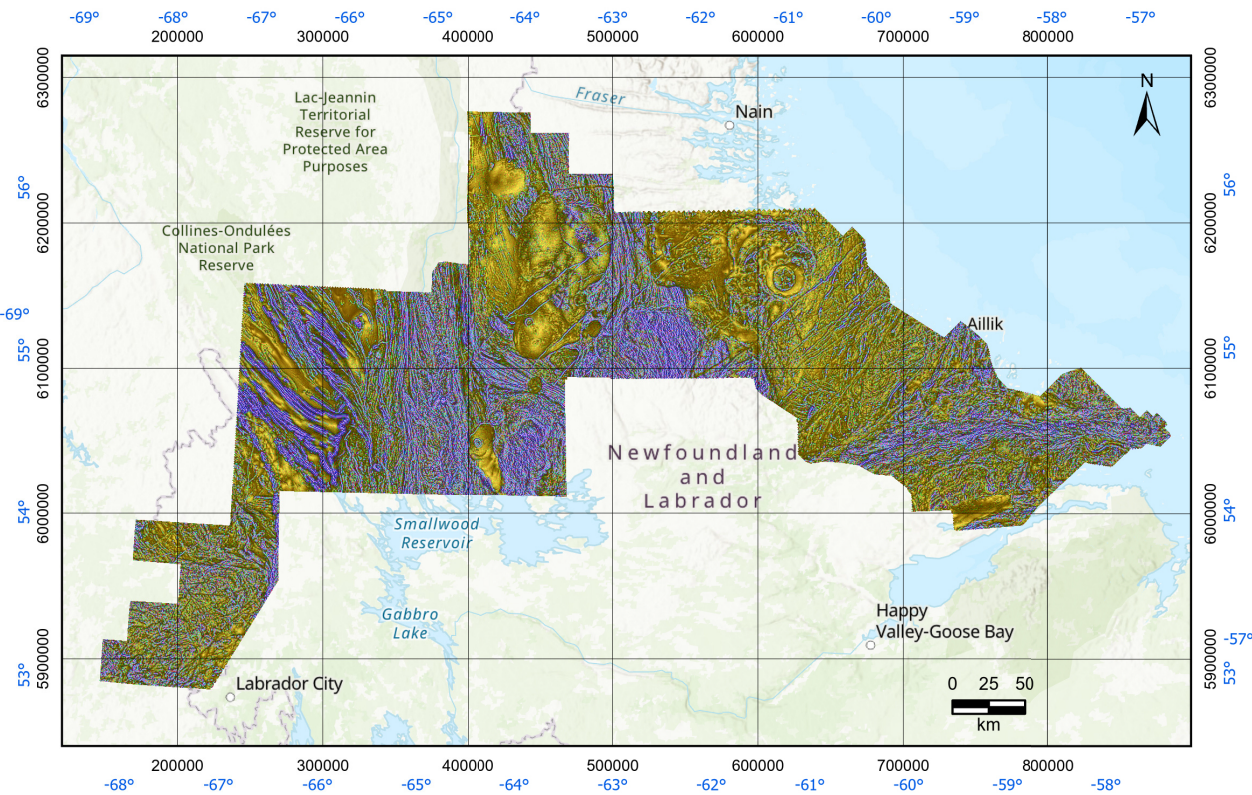


**Figure 16.** Enhancing aeromagnetic data by integrating grids technique, high-pass and low-pass filtering with tilt angle.

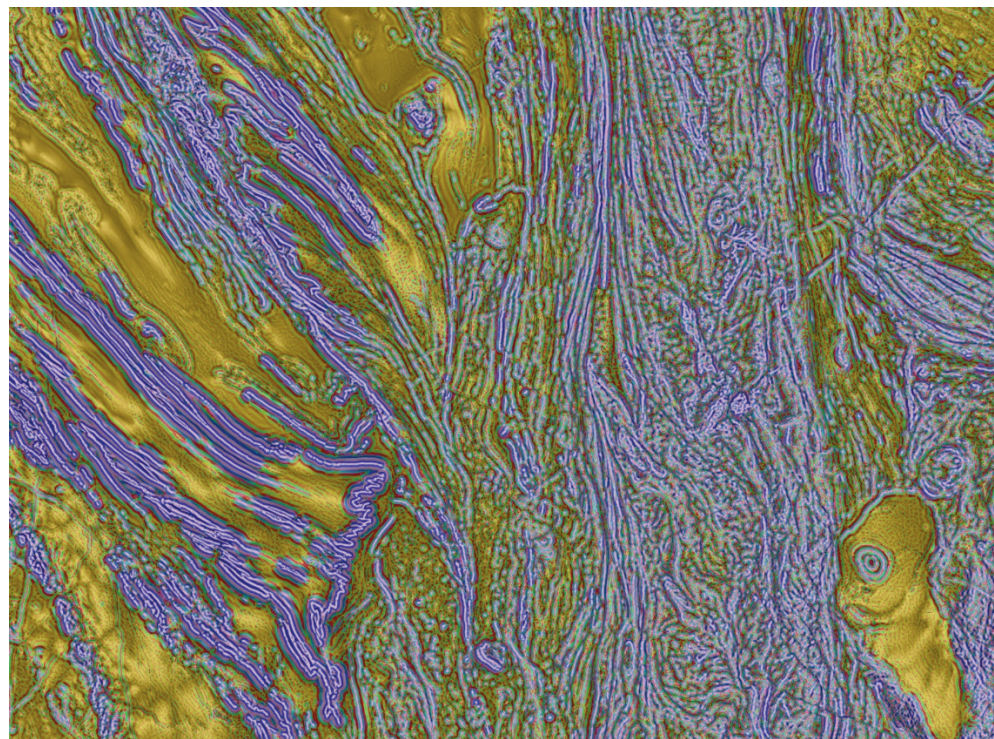


**Figure 17.** The combined aeromagnetic viewing depicts deeper and shallower structural components in one image, in the Southeastern Churchill Province, north of the Smallwood Reservoir.

pass) with 80% transparency. This subtle addition of colour variation aids in distinguishing geological domains, providing a balanced and enriched dataset that effectively delineates both regional and local magnetic anomalies for enhanced structural interpretation (Figures 18 and 19). The use of transparency and histogram-equalized stretches ensures that subtle features are not missing. It allows interpreters to emphasize specific elements, such as short-wavelength anomalies, without losing broader trends.

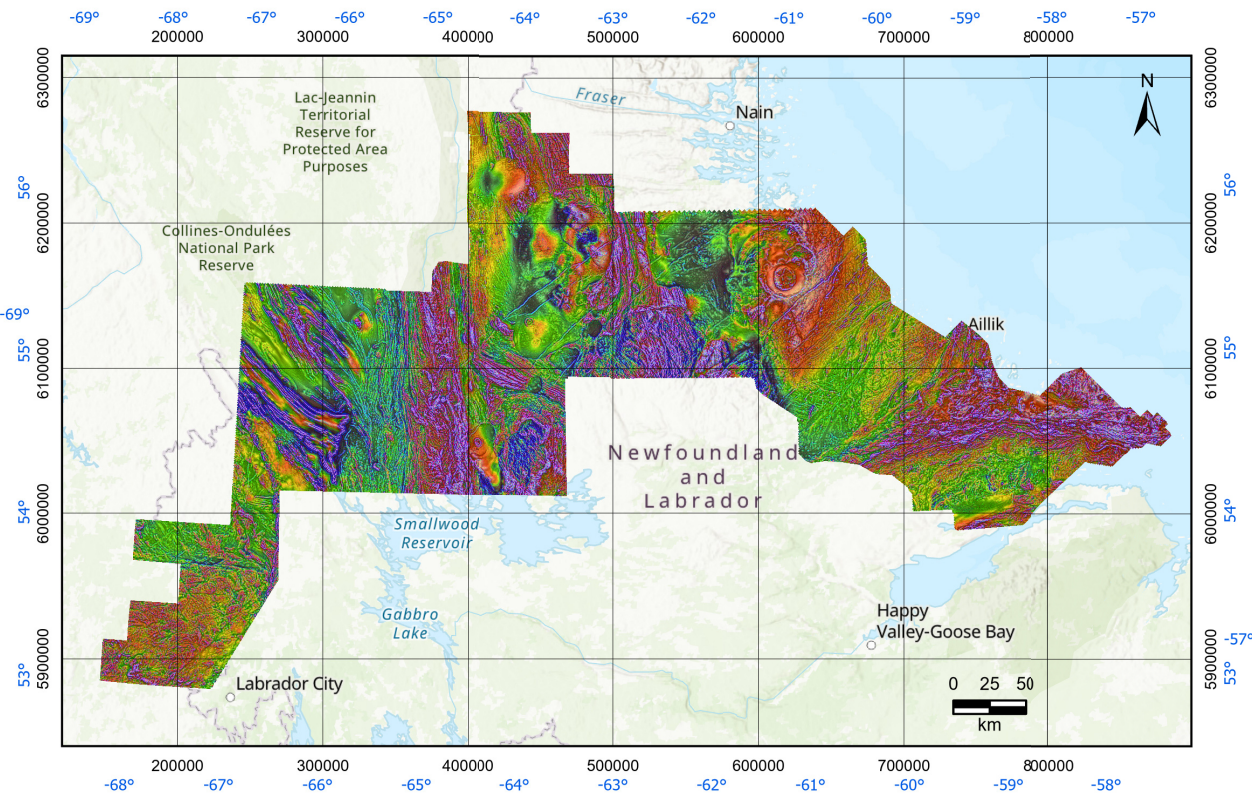
## COMPARING VARIOUS PROCESSED VIEWS

The comparison of frequency-domain processed magnetic imageries – 1VD, low-pass, high-pass and combined images (low pass, high-pass and tilt angle of low-pass) – reveals their unique strengths and limitations for geological interpretation. The 1VD grid is highly sensitive to shallow features, such as faults and dykes, offering excellent boundary definition but losing regional and deep-seated information. Low-pass filters excel at capturing deep, regional

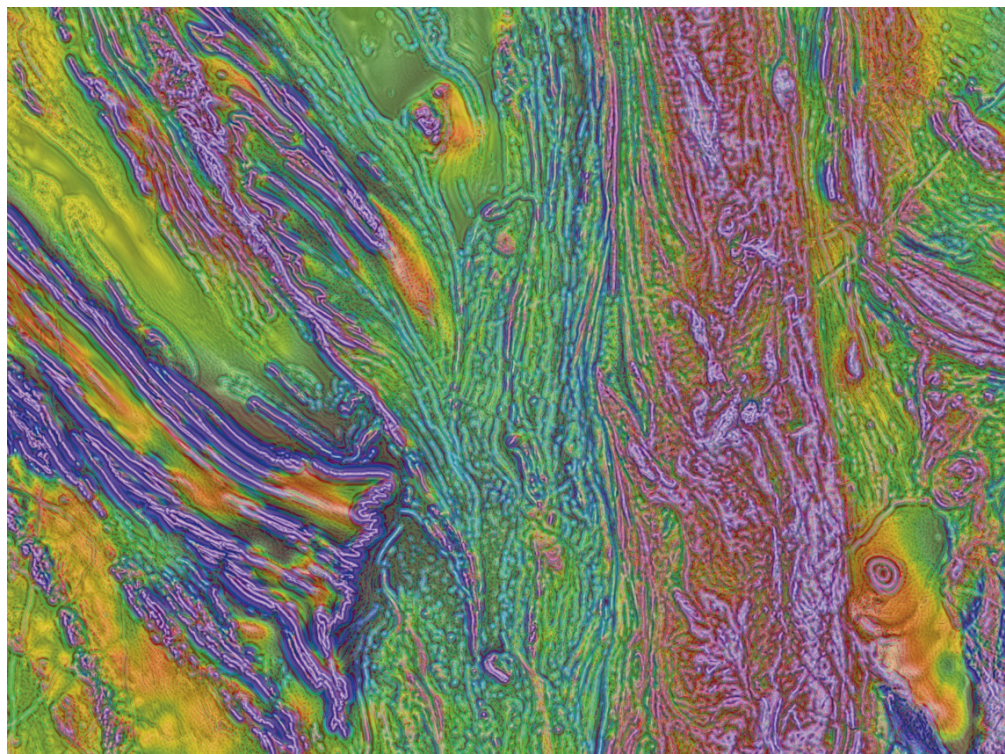
structures by suppressing noise and short-wavelength components, although they fail to highlight near-surface anomalies. High-pass filters, in contrast, isolate short-wavelength features, making them ideal for mapping shallow structures but at the cost of regional context and increased susceptibility to noise. The combined grid approach integrates the advantages of these methods by preserving both shallow and deep features, restoring regional context with the tilt angle of low-pass data, and enhancing boundary clarity with transparency and colour-coded visualization. As a result, the choice of method should align with the geological question at hand and the scale of interest.

Figure 20 presents a comparison between 1VD, low-pass, high-pass and combined images (low-pass, high-pass and tilt angle of low-pass) of magnetic data for the Southeastern Churchill Province.

Table 2 describes the limitations and advantages of these techniques for better understanding.



**Figure 18.** Enhancing aeromagnetic data by using the low-pass grid 80% transparent superposing onto the integrated image of high-pass and low-pass filtering with tilt angle.



**Figure 19.** The low-pass grid 80% transparent superposing onto the integrated image for the Southeast Churchill Province to depict short-wavelength anomalies, while retaining the long-wavelength anomalies.

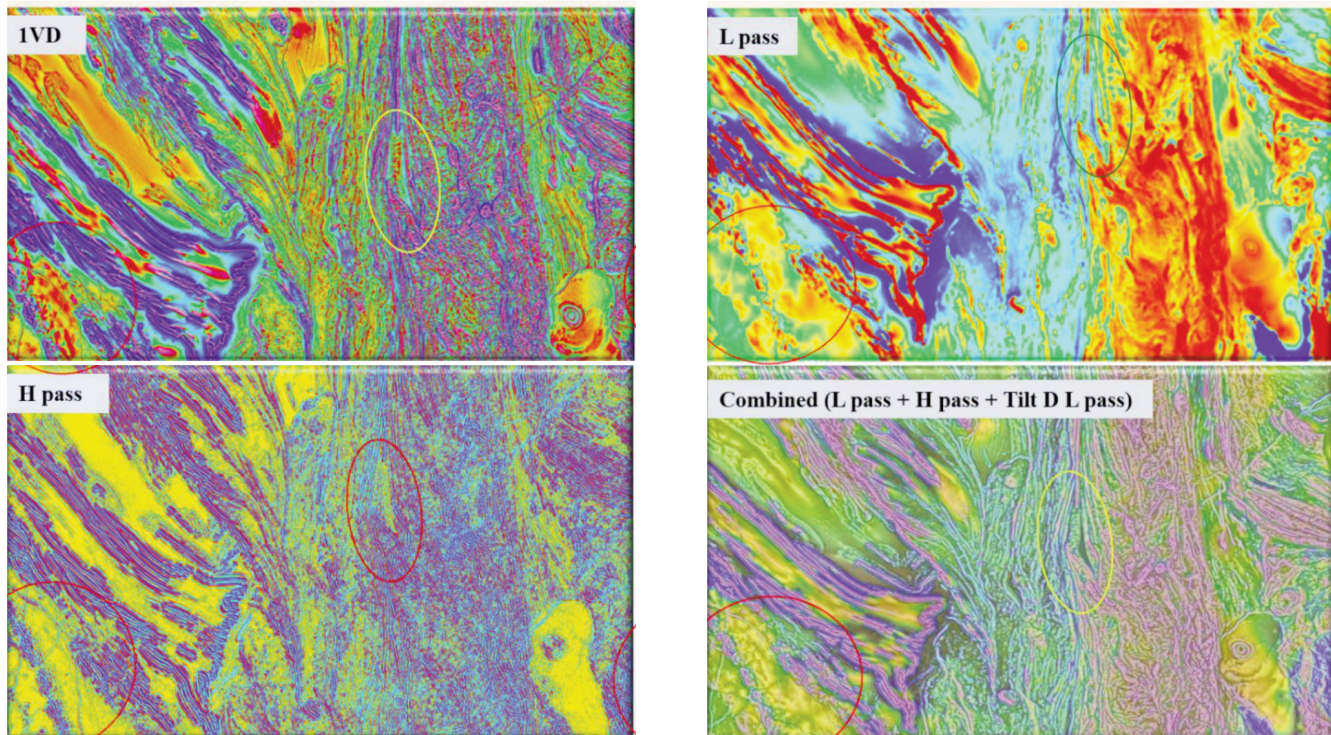


**Figure 20.** Comparing different processed magnetic data.

**Table 2.** Key comparisons

Method	Focus	Best For	Limitations
1VD	Shallow, high-frequency features	Faults, dykes and edges of bodies	Ignores deep-seated features; noisy
Low-Pass Filter	Long-wavelength (regional) anomalies	Regional geology, crustal structures	Masks near-surface features
High-Pass Filter	Short-wavelength (local) anomalies	Localized structures, ore deposits	Loses regional context; amplifies noise
Combined images	Multi-scale (local + regional)	Integrated geological interpretations	Computationally complex; requires skill

**REFERENCES**

Alken, P., Thébault, E., Beggan, C. D., Amit, H., Aubert, J., Baerenzung, J. and Zhou, B.  
 2021: International geomagnetic reference field: The thirteenth generation. *Earth, Planets and Space*, Volume 73, pages 1-25.

Briggs, I.C.  
 1974: Machine contouring using minimum curvature. *Geophysics*, Volume 39(1), pages 39-48.

Butler, J.P.  
 2019: New observations from the Andre Lake area (NTS 23I/12), western Labrador: Tectonic relationships in the hinterland of the New Québec Orogen. *In Current Research. Government of Newfoundland and Labrador, Department of Natural Resources, Geological Survey, Report 19-1*, pages 131-146.

Campbell, I., Saul, S., Isles, D. and Pridmore, D.  
 1992: Case studies in the application of the reduction to pole operator in aeromagnetic surveys. *9th Geophysical Conference and Exhibition Handbook. Abstracts. Australian Society of Exploration Geophysicists*, pages 25-26.

Cooper, G. R. J., and Cowan, D. R.  
 2006: Enhancing potential field data using filters based on the local phase. *Computers and Geosciences*, Volume 32(10), pages 1585-1591.

Cowan, D.R. and Cowan, S.  
 1993: Separation filtering applied to aeromagnetic data. *Exploration Geophysics*, Volume 24(3/4), pages 429-436.

Coyle, M.  
 2019: Aeromagnetic survey of the Hopedale area, Newfoundland and Labrador, parts of NTS 13-M/north and 13-N/north. *Geological Survey of Canada, Open File 8513 and Government of Newfoundland and Labrador, Department of Natural Resources, Geological Survey, Open File LAB/1737*.  
<https://doi.org/10.4095/313295>

Foss, C.  
 2020: Magnetic data enhancements and depth estimation. *Encyclopedia of Solid Earth Geophysics*, pages 1-14.

Isles, D.J. and Rankin, L.R.  
 2013: *Geological Interpretation of Aeromagnetic Data*. Published by Australian Society of Exploration Geophysicists, 351 pages

Jessell, M. W.,  
 2001: *An Atlas of Structural Geophysics II: Journal of the Virtual Explorer*.  
<http://virtual explorer.com.a4/2001/volume5>

Korhonen, J.V., Faihead, J.D., Hamoudi, M., Lesur, V., Mandea, M., Maus, S. and Thebault, E.  
 2007: *Magnetic Anomaly Map of the World—Carte des anomalies magnétiques du monde*.

Miller, H.G. and Singh, V.  
 1994: Potential field tilt—a new concept for location of potential field sources. *Journal of Applied Geophysics*, Volume 32(2-3), pages 213-217.

Morgan, R.  
 1998: Magnetic anomalies associated with the North and South Morecambe fields, U.K. *In Geologic*

Applications of Gravity and Magnetics. Published by Society of Exploration Geophysicists.

O'Connell, M.D. and Owers, M.  
2008: A line spacing compression method and an improved minimum curvature operator for grid interpolation of airborne magnetic surveys. *Exploration Geophysics*, Volume 39(3), pages 148-154.

O'Connell, M.D., Smith, R.S. and Vallee, M.A.  
2005: Gridding aeromagnetic data using longitudinal and transverse horizontal gradients with the minimum curvature operator. *The Leading Edge*, Volume 24(2), pages 142-145.

Spector, A. and Grant, F.S.  
1970: Statistical models for interpreting aeromagnetic data. *Geophysics*, Volume 35(2), pages 293-302.

Wardle, R.J., Gower, C.F., Ryan, B., Nunn, G.A.G., James, D.T. and Kerr, A.  
1997: Geological map of Labrador. Scale: 1:1 000 000. Government of Newfoundland and Labrador, Department of Mines and Energy, Geological Survey, Open File LAB/1226.